# Effect of Mg content and solution treatment on the microstructure of Al-Si-Cu-Mg alloys

ISMELI ALFONSO*, CUAUHTEMOC MALDONADO, GONZALO GONZALEZ, ARNOLDO BEDOLLA
*Instituto de Investigaciones Metalurgicas, Universidad Michoacana de San Nicolás de Hidalgo, Edificio U. Cividad Universitaria, Morelia, Michoacana, Mexico C.P. 58000*
*E-mail: post18@jupiter.umich.mx*

**Published online:** 2 March 2006

Three different quaternary alloys Al-6Si-3Cu-xMg ($x = 0.59$, 3.80 and 6.78 wt.%) were produced using conventional ingot casting metallurgy. The study was focused to investigate the effect of magnesium and solution heat treatment on the microstructure. Results shown variations in composition and morphology for the silicon-rich phases as well as a change of the predominant copper-rich phase $Al_2Cu$ ($\theta$) to $Al_5Cu_2Mg_8Si_6$ (Q phase) when magnesium content is increased. The amount of Mg in solid solution was constant for the three different cast-alloys, increasing considerably after solution heat treatment to 2.7 at.% for the alloy with higher Mg content This fact allowed to obtain Cu:Mg ratios (in at.%) in solid solution lower than 1.0 for the alloys with 3.80 and 6.78 Mg wt.%, impossible to reach for the alloy with low Mg content. During dissolution process, $Al_2Cu$ phase was observed to be more suitable to dissolve than Q phase. Fragmentation, spheroidization and coarsening of Q and silicon-rich phases were observed. Solution time required for these processes occurrence was longer for Q phase. Solution heat treatments at 480°C for 12 h were found to be appropriate for the studied alloys.


## 1. Introduction

One common material for engine applications is the Al-Si-Cu-Mg 319 alloy. This quaternary alloy has good castability, excellent corrosion resistance and machinability, medium strength, and low specific weight. Its silicon content ranges from 5.5 to 6.5 (wt.%), and copper varies from 3.0 to 4.0 (wt.%). The presence of magnesium improves strain, hardenability and enhances the material strength by solid solution [1]. Chemical composition and heat treatment exert an important influence on the mechanical properties. The most applied heat treatment for this alloy is a solution treatment followed by an age-hardening that is required for the precipitation of the $Al_2Cu$ hardening constituent. Solution heat treatment is particularly suitable for alloys with high magnesium content in order to promote the formation of the important strengthening precipitate, $Mg_2Si$. Ouellet *et al.* [2] report a hardening peak caused by a cooperative precipitation of $Al_2Cu$ and $Mg_2Si$ phases in this kind of alloys. It has been found that precipitation in the Al-Cu-Mg-Si alloys depends on magnesium contents as well as on the Cu:Mg ratio in solid solution. For a Cu:Mg ratio of 2.0 (at.%), preferential precipitation of $Mg_2Si$ occurs, while a ratio close to 8.0, promotes the formation of the $Al_2Cu$ compound [3]. The increase of magnesium content in solid solution contributes to the precipitation phenomenon since clusters of magnesium are the precursors in the formation of $Mg_2Si$ in Al-Mg-Si alloys [4]. It has been observed that high magnesium levels promote the precipitation process. However, these effects of magnesium in quaternary Al-Si-Cu-Mg alloys have not been examined in detail.

Prior to the study of the precipitation hardening process it is necessary to examine the solution stage of the heat treatment. There are some previous works on characterization and dissolution for Al-Si-Cu-Mg alloys using low (<1.0 wt.%) magnesium contents [2, 5–8], but there is no much research work on this alloy with magnesium contents higher than 1.0 wt.%. Solution heat treatment exerts an important influence on the precipitation process and for Al-Si-Cu-Mg alloys the solution temperature must be controlled within a narrow range, due to the presence of low melting point copper-rich phases. The as-cast structure of the 319 alloy includes $\alpha$-aluminium, silicon eutectic particles, $Mg_2Si$, $Al_2Cu$, $Al_5Cu_2Mg_8Si_6$ and other complex

*Author to whom all correspondence should be addressed.
0022-2461 
DOI: 10.1007/s10853-006-4494-y

intermetallic compounds [2, 5]. The precipitation sequence from liquid [6, 7] shows that the last precipitation reaction occurs close to 507 °C, where the precipitation temperature depends mainly on chemical composition. However, the reported solution temperature range is wide. In Al-Si-Cu-Mg alloys with low magnesium content (0.5 wt.%), Ouellet *et al*. [2] used a solution temperature of 500 °C because at 505 °C fusion of low melting point phases can occur, while Wang *et al*. [9] reported that for a similar alloy with a solution temperature of 520°C mechanical properties are increased without localized melting. That is why a temperature lower than 500°C is safe enough for avoiding localized melting. The principal aim of the present paper is to examine the effect of an increase in magnesium content on the microstructure, and the relationship between solution heat treatment and dissolution of second phases in Al-Si-Cu-Mg alloys. This information is important because the dissolution process directly affects mechanical properties of the as-quenched alloy, due to the influence of microstructural parameters such as size and morphology of second phases. Dissolution process indirectly affects the mechanical properties of the alloy because of the effect that solution treatment exerts on the precipitation hardening mechanism. Keeping this purpose in mind, optical microscopy (OM) and scanning electron microscopy (SEM) were carried out on experimental Al-Si-Cu-xMg alloys, in order to investigate the effects of magnesium and solution treatment on phase formation and dissolution.

## 2. Experimental

A 356 alloy ingot, with Al-8.5Si-0.3 Mg (wt.%) was used as a master-alloy in conventional melting of the experimental alloys. Pure copper powder (>99.9% purity) and magnesium ingot (>99.9% purity) were added to the base alloy in order to obtain three alloys with different magnesium contents. The alloys were produced in a Leybold-Heraeus induction furnace with a controlled argon atmosphere. A graphite crucible was used and the melting temperature was kept in the range of 750°C ± 10°C. The molten alloys were poured into a conventional mould without preheating inside the furnace chamber to avoid pore formation and metal oxidation. Chemical composition for the experimental alloys is shown in Table I. The experimental alloys in the as-cast condition were characterized using OM and SEM. Optical microscopy and scanning electron microscopy examination were carried out in a Nikon EPIPHOT 300 and a JEOL JSM 6400 respectively. SEM was operated at 20 kV. Using standard metallographic techniques, specimens for OM and SEM were polished and etched in a 10 mL $H_3PO_4$ – 90 mL $H_2O$ solution at 40°C during one minute for optimum examination of second phases.

Forty cubic samples (1.0 × 1.0 × 1.0 cm) were sectioned from each alloy ingot. Five samples per composition were mounted and polished to 0.05 $\mu$m. The remaining samples were solution heat treated at 480 ± 3 °C in a forced-air furnace with different solution times, i.e. 4, 8, 12, 20, 30, 48 and 72 h (five samples per batch). It should be noticed that the selected solution temperature is lower than the critical dissolution temperature, for which localized melting has been observed in similar alloys [2, 6]. After solution treatment, the samples were quenched in hot water (60 °C) to freeze the microstructure. These samples were mounted and polished following the same procedure applied to the as-cast specimens and were examined using OM and SEM to observe microstructural changes.

TABLE I Chemical composition (wt.%) of the experimental alloys studied in the present work

| Alloy code | Si | Cu | Mg | Fe | Mn | Zn | Ti | Al |
|---|---|---|---|---|---|---|---|---|
| AM01 | 6.40 | 3.02 | 0.59 | 0.34 | 0.09 | 0.04 | 0.01 | Balance |
| AM03 | 6.31 | 3.03 | 3.80 | 0.32 | 0.08 | 0.03 | 0.13 | Balance |
| AM06 | 5.84 | 2.95 | 6.78 | 0.31 | 0.07 | 0.03 | 0.12 | Balance |

## 3. Results and discussion

### 3.1. As-cast alloys

No cast defects were observed in the experimental alloys which could be linked to an increase in magnesium content, as shown in Fig. 1a–f. Optical microscopy of the specimen AM01 (0.59 Mg wt.%) (Fig. 1a), shows the presence of a dark fibrous silicon eutectic and a copper-rich intermetallic phase that precipitates during solidification either as a block-like $Al_2Cu$ or as a eutectic (Al + $Al_2Cu$). In addition to these phases, a small presence of quaternary $Al_5Cu_2Mg_8Si_6$ (Q) phase was also detected. Using OM the silicon-rich and $Al_5Cu_2Mg_8Si_6$ (Q) phases look as dark grey or black phases. It should be noticed that the $Al_2Cu$ phase cannot easily be resolved because it appears slightly darker than the $\alpha$-aluminium. In order to overcome this difficulty, scanning electron microscopy was applied in the backscattered mode (see Fig. 1b). As can be seen in Fig. 1c–f important microstructural changes occur for the alloys AM03 (3.80 Mg wt.%) and AM06 (6.78 Mg wt.%) compared to AM01 (0.59 Mg wt.%). The microstructure shown a significant presence of Q phase instead of $Al_2Cu$, and it is observed that besides few quantity of localized eutectic silicon phase, silicon is predominantly as an irregular black phase. Microanalysis by EDS shown that the eutectic silicon phase contains approximately 30 Si at.%, while in the experimental alloys AM03 (3.80 Mg wt.%) and AM06 (6.78 Mg wt.%) the irregular silicon-rich phase contains more than 90 Si at.%. Volume percentage of copper-rich phases increased from 11.45 to 22.5% when magnesium content increased from 0.59 to 6.78 wt.%. Just a small amount of block-like $Al_2Cu$ grow up from the $Al_5Cu_2Mg_8Si_6$ in alloys AM03 (3.80 Mg wt.%) and AM06 (6.78 Mg wt.%), while copper-rich phases segregated away from the silicon-rich phases.

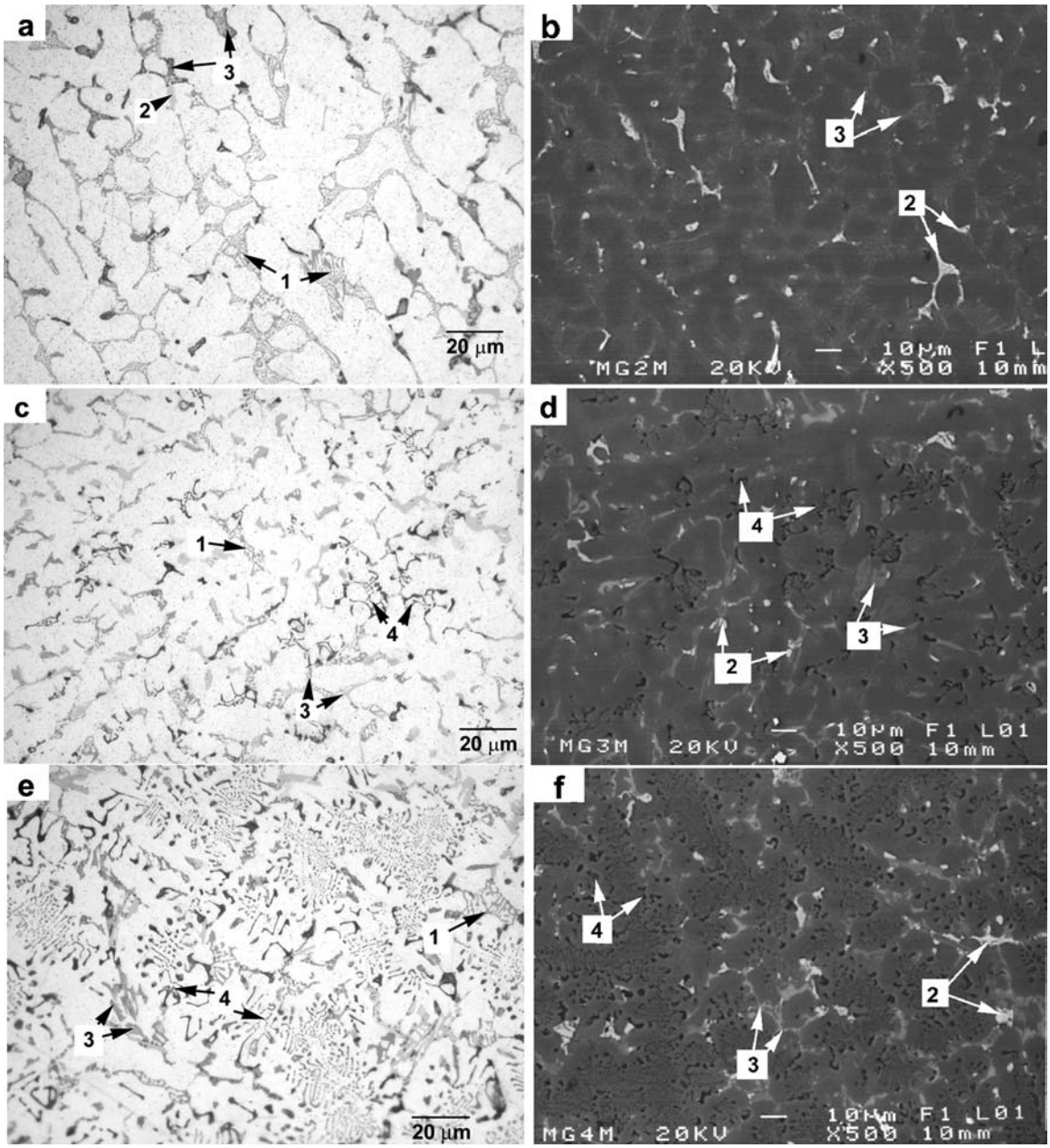


*Figure 1* Optical (left) and SEM-backscattered electrons (right) micrographs of the as-cast alloys illustrating the most representative phases for alloys. (a, b) AM01 (0.59 Mg wt.%), (c, d) AM03 (3.80 Mg wt.%) (e, f) AM06 (6.78 Mg wt.%). [1: eutectic silicon, 2: $Al_2Cu$, 3: $Al_5Cu_2Mg_8Si_6$, 4: silicon].

## 3.2. Solubilization

The evolution of microstructure in the AM01 (0.59 Mg wt.%) alloy solution heat treated at 480 °C for solution times of 4–72 h, is described in Fig. 2a–d. For specimens solution treated during 4 h (see Fig. 2a), the $\alpha$-aluminum dendritic structure remains unchanged, with a slight tendency to silicon-particle fragmentation. The dendritic structure disappeared completely after 30 h of solution treatment (see Fig. 2c). Disintegration of the fibrilar silicon eutectic structure in small particles is followed by spheroidization and coarsening. Apparently, both processes occur simultaneously. For a solution time as short as 4 h (see Fig. 2a) all Q phase dissolved, while dissolution of $Al_2Cu$ is extensive, nevertheless even after a solution time of 72 h dissolution of $Al_2Cu$ is incomplete, leaving tiny particles localized at the border of silicon eutectic particles, see Fig. 2d.

Decomposition of the fibrous silicon eutectic phase into small spherical particles in short times (1 min) has been reported by Ogris *et al.* [10] for Al-Si-Mg alloys. The unstable shape of fibrous silicon eutectic was explained by Lord Rayleigh in 1878 [11]. The driving force for this process is the reduction of the surface energy. The growth process of the silicon eutectic particles can be described by the Ostwald ripening of precipitates, where pure Ostwald ripening means that bigger particles grow at the expense of smaller particles [10]. Coarsening is attributed to residual particles produced during the dissolution process [7]. It

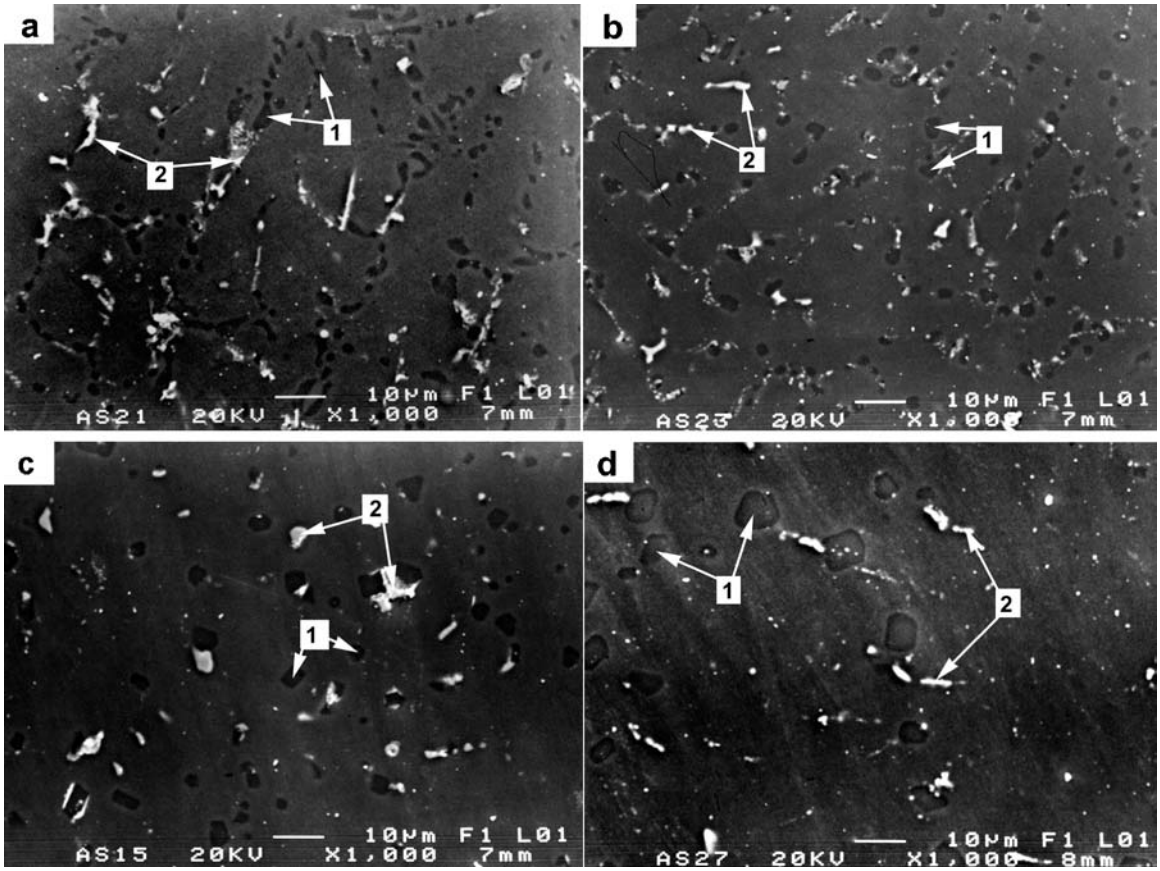


*Figure 2* SEM-backscattered electrons micrographs showing evolution of the microstructure in the alloy AM01 (0.59 Mg wt.%) solution treated at 480 °C. (a) after 4 h, (b) after 12 h, (c) after 30 h, (d) After 72 h. [1: eutectic silicon particles, 2: $Al_2Cu$ phase].

is important to consider that the dissolution stage must have two important objectives: (1) firstly, to maximize the content and distribution of magnesium, copper and silicon in solid solution, and (2) secondly, decrease the aspect ratio and increase the size and spacing between particles. The first objective is important because it is the optimum condition for a good ageing process and obtaining maximum yield strength. The second objective is important for an increasing ductility [7].

The microstructural evolution with solution time in the AM03 (3.80 Mg wt.%) alloy solution heat treated at 480 °C for times of 4–72 h is shown in Fig. 3a–d. Compared to the AM01 (0.59 Mg wt.%) alloy, is clearly seen that the amount of undissolved copper-rich phases in the AM03 (3.80 Mg wt.%) alloy was higher. This result should be expected because the main second phase is Q instead of $Al_2Cu$, and Q is reported as a phase with low solubility in solid solution [2], being insoluble at solution temperatures as high as 530 °C [13], while dissolution of the eutectic Al + $Al_2Cu$ takes place at temperatures close to the end of the solidification temperature range (approximately 480 °C). In alloy AM03 (3.80 Mg wt.%) the irregular silicon phase and $Al_2Cu$ dissolve completely after 4 h of solution heat treatment. In this case, the quaternary phase undergoes fragmentation, spheroidization and coarsening, similar to the process observed for the eutectic silicon present in AM01 (0.59 Mg wt.%) alloy. Solution time required for the Q phase fragmentation is near to 12 h (Fig. 3b), while spheroidization occurs after 30 h (Fig. 3c). These longer times compared to eutectic silicon present in AM01 alloy can be explained from theoretical considerations which indicate that interfacial instabilities cannot readily occur in plate-like phases as Q and hence the structure is resistant to fragmentation and spheroidization [12]. However, fibrous eutectic phases are susceptible to changes in shape.

The effect of solution treatment on the microstructure of the AM06 (6.78 Mg wt.%) alloy at 480 °C for solution times of 4–72 h is described in Fig. 4a–d. It is observed that all $Al_2Cu$ is dissolved after a solution treatment of 4 h. Total dissolution of irregular Si-rich phase was not possible for this alloy, showing complete fragmentation and spheroidization after a solution time of 4 h. Under these experimental conditions the Q phase follows the same behaviour observed in AM03 (3.80 Mg wt.%) alloy, presenting fragmentation, spheroidization and coarsening after 12 h of solution heat treatment.

The changes in the volume percent of undissolved copper-rich phases for all alloys at different heat treatment times are shown in Fig. 5. In AM01 (0.59 Mg wt.%) alloy the decrease of undissolved copper-rich phases ($Al_2Cu$ for this alloy) shows a drop. Taking the as-cast condition

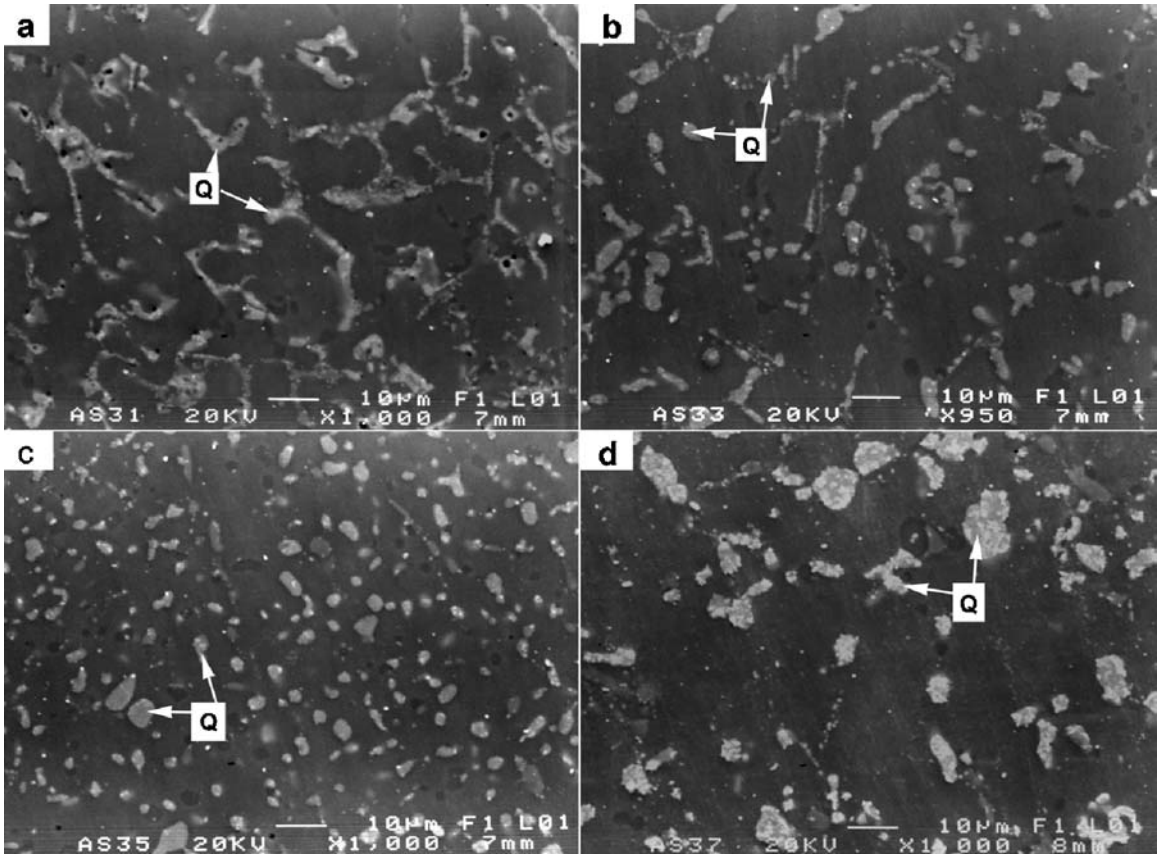


*Figure 3* SEM-backscattered electrons micrographs showing evolution of the microstructure in the alloy AM03 (3.80 Mg wt.%) solution treated at 480 °C. (a) after 4 h, (b) after 12 h, (c) after 30 h, (d) after 72 h. [Light Q phase is well observed].

as the initial value (100%), the volume percent of undissolved $Al_2Cu$ after 12 h, when equilibrium was reached, is 53%. For the alloy AM06 (6.78 Mg wt.%) the undissolved Q phase quantity for 12 h is near to 70%, while for the alloy AM03 (3.80 Mg wt.%) dissolution of Q phase is less than 10% and the drop and the posterior equilibrium is not clearly observable as for AM01 and AM06 alloys. This result can be explained due to the fact that Q phase is less soluble than $Al_2Cu$.

Since morphology, size and spatial distribution of second phases are important for the mechanical properties of an alloy, it is convenient to have a parameter for describing changes on these particular microstructural features. The selected parameters were equivalent diameter, inter-particle spacing and shape factor, which are depicted in Fig. 6a–c. The equivalent diameter ($D_e$) is a parameter related to particle size and is defined as the diameter of a circle with equivalent area [10] and is given by Equation 1 where $A_p$ is the particle area and n the number of measured particles:

$$D_e = \frac{1}{n} \sum \left( \frac{4A_p}{\pi} \right)^{1/2} \quad (1)$$

The change in $D_e$ for the particles present in the experimental alloys is shown in Fig. 6a. Particles present in the AM01 (0.59 Mg wt.%) alloy after 72 h of solution heat treatment correspond to silicon eutectic, for which $D_e$ increases from 2.0 $\mu m^2$ at 4 h to 6.2 $\mu m^2$ at 72 h due to the ripening process. For solution times in the range from 48 h to 72 h, the parameter $D_e$ remains without noticeable changes, fact that can be explained because of the absence of small particles required for the ripening process. The evolution of $D_e$ for Q phase particles present in AM03 alloy is quite different. A steady growth process like in the silicon-rich phases is not observed, but an alternated fragmentation and coarsening process take place. For the AM06 alloy, Si particles and Q phase were analyzed. Average diameter behaviour for Si particles is similar to the observed for Si eutectic particles present in AM01 alloy, increasing until 48 h and remaining without noticeable changes for further times. Equivalent diameter for Q phase does not increase in a continuous way due to that coarsening happens after fragmentation, decreasing the size of the segments at 20 h. For the experimental alloys the parameter $D_e$ for silicon-rich particles is much smaller than for the Q particles because of the sequence of fragmentation, coarsening and spheroidization processes are different. The Q structure is not very suitable for shape changes and that is why it cannot be easily fragmented into smaller particles.

Fig. 6b shows the change in the average inter-particle spacing as a function of solution time at 480 °C. This

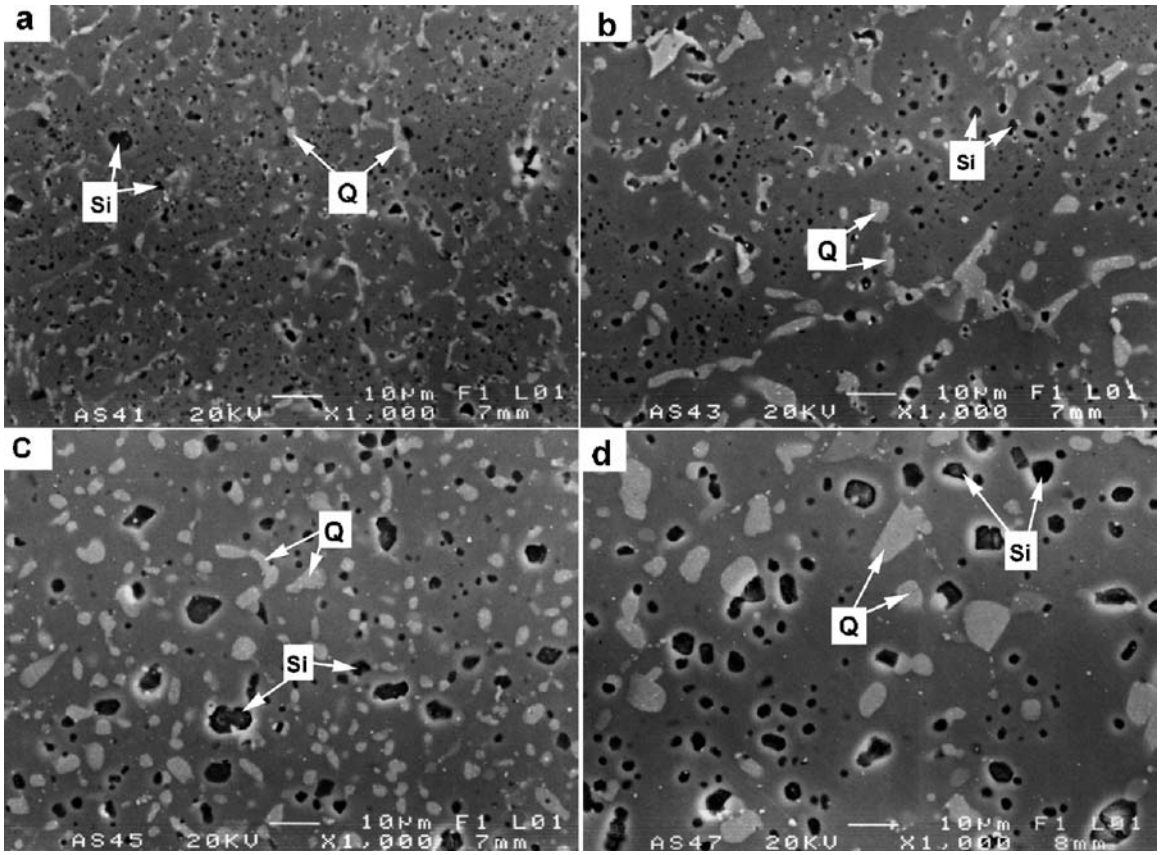


*Figure 4* SEM-Backscattered electrons micrographs showing evolution of the microstructure in the alloy AM06 (6.78 Mg wt.%) solution treated at 480 °C. (a) after 4 h, (b) after 12 h, (c) after 30 h, (d) after 72 h. [Black silicon irregular phase (Si) and light quaternary phase (Q) are well observed].

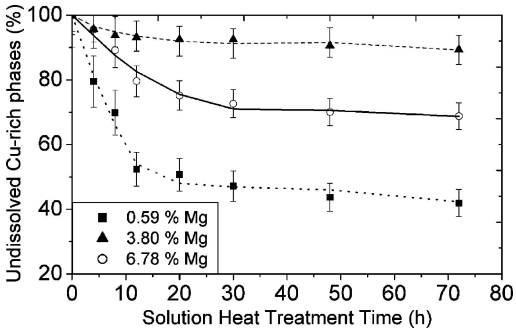


*Figure 5* Variation in the percentage in volume of undissolved copper-rich phases as a function of solution treatment time at 480 °C for the alloys with 0.59, 3.80 and 6.78% Mg.

parameter was calculated taking into account all the present particles in each alloy. Inter-particle spacing increase in all experimental conditions, in agreement with observations made during the analysis of phase dissolution and equivalent diameter behaviour, corresponding to the increase in size and the decrease in the number of particles. The increment in inter-particle spacing becomes slower for longer solution times because the particle growth is slower. The average inter-particle spacing increased to 9.0 $\mu$m for AM01 alloy (0.59 Mg wt.%) reaching approximately 6.0 $\mu$m for AM03 (3.80 Mg wt.%) and 5.0 $\mu$m for the AM06 (6.78 Mg wt.%) alloy. This decrease for alloy AM06 can be explained due to the presence of two kind of particles (silicon-rich and Q) instead of only one as in alloy AM01 (eutectic silicon) and alloy AM03 (Q), besides the higher percentage of second phases in alloys AM03 and AM06 alloys compared to AM01 alloy.

Fig. 6c shows the change in the average shape factor (F) at different solution treatment times at 480 °C. This dimensionless parameter is defined in Equation 2, where $A_p$ is the area, $P_p$ is the perimeter and $n$ the number of measured particles.

$$F = \frac{1}{n}\sum\left(\frac{4\pi A_p}{P_p^2}\right) \tag{2}$$

A perfect circle will have a shape factor of 1, while the shape factor of a line will approach to zero. Particles analyzed are silicon eutectic present in the AM01 (0.59 Mg wt.%) alloy, Q phase particles present in AM03 (3.80 Mg wt.%) alloy and Si particles and Q phase present in AM06 (6.78 Mg wt.%) alloy. Spheroidization of all phases is observed with an increasing solution time. Silicon-rich phases show spheroidization levels near to 0.5 with solution times as short as 4 h, while for Q phase the shape factor is lower than 0.4 for solution times as long as 72 h. This result indicates that while spheroidization of silicon-rich phases occurs instantaneously, Q phase spheroidization needs longer solution times, fact that can be explained due to considerations of phase surface energy.

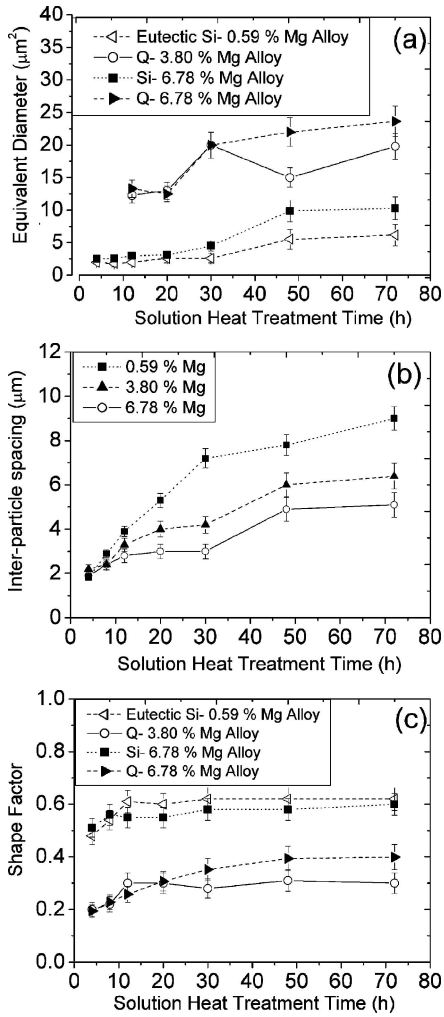


*Figure 6* Variation of average particles equivalent diameter (a), inter-particle spacing (b) and shape factor (c) at 480 °C for solution times of 4–72 h for Q and Si-rich particles in AM01 (0.59% Mg), AM03 (3.80% Mg) and AM06 (6.78% Mg) alloys.

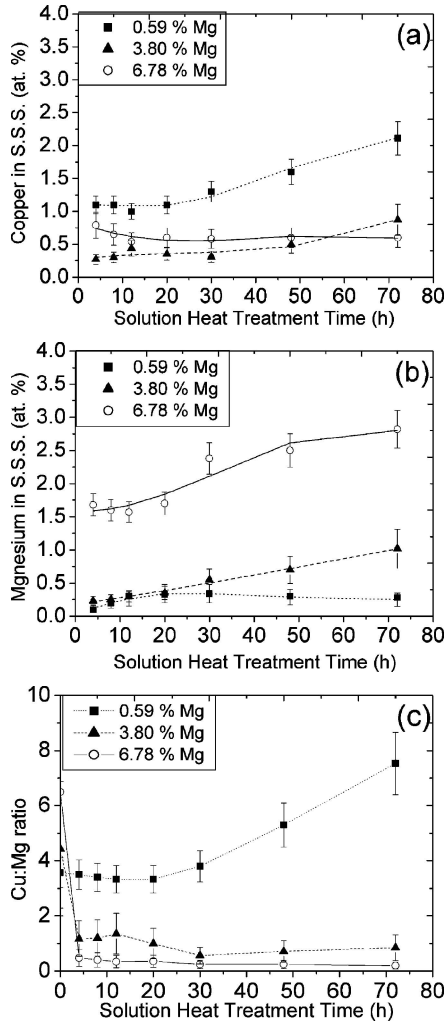


*Figure 7* Variation of the average atomic percentage of copper (a) and magnesium (b) in the supersaturated solid solution (S.S.S) as a function of solution treatment time at 480 °C for alloys AM01 (0.59% Mg), AM03 (3.80% Mg) and AM06 (6.78% Mg). (c) Variation in the average Cu:Mg ratio (in at.%).

The change in the average atomic percent of copper and magnesium in solid solution at 480 °C is described in Fig. 7a–b. The most important change in the quantity of Cu in solid solution is for the AM01 alloy, as can be seen in Fig. 7a, due to the dissolution of the Cu-rich $Al_2Cu$ phase, reaching 2.0 at.% of Cu after 72 h. For the as-cast alloys magnesium content remained almost constant (near to 0.1 wt.%), which agrees with results reported by Li *et al.* [5] for alloys with lower magnesium content (<1.0 wt.%). After heat treatment important increases in the quantity of Mg in solid solution were observed for the alloys with 3.80 and 6.78 wt.% Mg (see Fig. 7b), reaching maximum values of 1.0 and 2.7 at.% respectively. This is an important result because different Cu:Mg ratios can be obtained in order to study the influence of these conditions on the precipitation process. Obtained Cu:Mg ratios in solid solution (in at.%) can be observed in Fig. 7c. As can be seen for the alloy with 0.59% Mg (AM01), Cu:Mg ratios are always higher than 3.5, reaching 8.0 at 72 h, while for the alloys with 3.80 and 6.78 wt.% of Mg, ratios reach values lower than 1.0. These results show that an important decrease in Cu:Mg ratios, due to an increase in magnesium in solid solution, can be obtained by selecting the adequate alloy chemical composition and solution heat treatment conditions.

## 4. Conclusions

The effect of magnesium content and the solution heat treatment on the microstructure of three quaternary Al-Si-Cu-Mg alloys containing 0.59, 3.80 and 6.78 wt.% of magnesium were studied. From the analysis of the results, the following conclusions can be drawn:

1. The increase of magnesium content in the alloys promotes Q phase formation. Dissolution of this phase is much more difficult than $Al_2Cu$ phase dissolution. Solution heat treatment time of 12 h at 480 °C is enough to obtain an important degree of dissolution of the phases in the studied alloys.

2. In the as-cast condition, magnesium content in solid solution does not vary for the examined compositions. For the alloys with 3.80 and 6.78% Mg the amount of Mg in solid solution can be increased after solution heat treatment and therefore, Cu:Mg ratios (in at.%) lower than 1.0 are obtained.

3. Fragmentation, spheroidization and coarsening occurred for silicon-rich phases and Q phase after the solution treatment. Solution time required for these processes to occur in Q phase is higher.


## Acknowledgements

The authors would like to thank F. Solorio, G. Lara and R.D. Cervantes for technical assistance and they also acknowledge the financial support provided by CIC and CGEP (UMSNH), México, and the material provided by Castech S.A. de C.V.


## References


1. J. E. HATCH, in "Aluminium, Properties and Physical Metallurgy" (American Society for Metals, USA, 1993) p. 232.
2. P. OUELLET and F. H. SAMUEL, *J. Mater. Sci.* **34** (1999) 4671.
3. R. M. GOMES, T. SATO and H. TEZUKA, *Mater. Sci. Forum Vols.* **217–222** (1996) 793.
4. M. MURAYAMA, K. HONO, M. SAGA and M. KIKUSHI, *Mater. Sci. and Eng. A* **250** (1998) 132.
5. Z. LI, A. M. SAMUEL, F. H. SAMUEL, C. RAVINDRAN and S. VALTIERRA, *J. Mater. Sci.* **38** (2003) 1203.
6. F. H. SAMUEL, *J. Mater. Sci.* **33** (1998) 2284.
7. G. Q. WANG, X. F. BIAN, W. M. WANG and J. Y. ZHANG, *Mater. Letters.* **57** (2003) 4083.
8. L. LASA and J. M. RODRIGUEZ-IBABE, *Mater. Charact.* **48** (2002) 371.
9. P. S. WANG, S. L. LEE and J. C. LIN, *J. Mater. Res.* **15** (2000) 2035.
10. E. OGRIS, H. LUCHINGER and P. J. UGGOWITZER, *Mater. Sci. Forum.* **396–402** (2002) 152.
11. E. WERNER. Z. METALLK. **81** (1990) 786.
12. J. W. MARTIN and R. D. DOHERTY, in "Stability of Microstructures in Metallic Systems" (Cambridge University Press, London, 1980).
13. A. K. GUPTA, A. K. JENA and M. C. CHATURVEDI, *Mater. Sci. Tech.* (1987) 1023.



*Received 9 February*
*and accepted 13 June 2005*